Limitations in the Synthesis of High Molecular Weight Polymers via Nitroxide-Mediated Controlled Radical Polymerization: Modeling Studies

Todd M. Kruse,[†] Razima Souleimonova,[†] Andrew Cho,[†] Maisha K. Gray,[‡] John M. Torkelson,[†,‡] and Linda J. Broadbelt*[,†]

Department of Chemical Engineering and Department of Materials Science and Engineering, Northwestern University, Evanston, Illinois 60208

Received February 5, 2003; Revised Manuscript Received June 12, 2003

ABSTRACT: The nitroxide-mediated controlled radical polymerization (NM-CRP) of styrene was modeled at the mechanistic level using the method of moments. The mechanistic models developed described the kinetics and the molecular weight development of the living free-radical polymerization process. A base model was constructed which included initiator decomposition, propagation, end-chain coupling, and termination by recombination and disproportionation. Using an Evans−Polanyi description of the activation energy ($E = E_0 + \alpha\Delta H_R$), the base model was fit to a set of experimental data for the living free radical polymerization of styrene at 87 °C[1] to obtain the heat of reaction for decoupling (ΔH_R for the di-*tert*-butyl nitroxide coupling agent) and to fit the intrinsic barrier (E_0) for propagation/depropagation. The remaining rate parameters were primarily obtained from the literature, while some were taken from previous modeling work in our laboratory.[2,3] The fit of the base model to the experimental data was then compared to the fit obtained when chain transfer to monomer and both chain transfer to monomer and styrene thermal initiation were included in the mechanism. It was found that including styrene thermal initiation was critical to being able to obtain good agreement between the model and the experimental data. The fitted parameters obtained after including styrene thermal initiation were E_0 for propagation/depropagation = 10.78 ± 0.08 kcal/mol and ΔH_R for the decoupling reaction = 22.70 ± 0.40 kcal/mol. Using these fitted parameters, the model was used to predict the evolution of M_n and M_w of the polymer product at different times and temperatures and with a macroinitiator. The importance of reactions such as chain transfer to polymer and the reaction between a nitroxide radical and a polymeric radical to form a hydroxy amine was also investigated, and it was found that these reactions were negligible.

Introduction

"Living", or controlled, free radical polymerization (LFRP) has received considerable attention in recent years due to the possibility that low-polydispersity polymers with predetermined molecular weights and novel architectures can be synthesized. During LFRP, the reversible termination of polymeric radicals with excess stable radicals such as nitroxides lowers the concentration of growing polymeric radicals in the system, which minimizes termination reactions such as combination and disproportionation. In this pseudo-living environment, most of the growing polymer chains live for approximately the same amount of time. As a result, their lengths are similar, and a polymer product with a low polydispersity index (PDI) is produced.

Three different LFRP approaches have been examined in the literature: nitroxide-mediated, metal-mediated, and atom transfer radical polymerization catalyzed by metals. These methods differ by the type of the coupling agent used. The use of nitroxides is one of the most widely studied controlled "living" free radical polymerizations.[4−16] Nitroxide-mediated controlled radical polymerization (NM-CRP) may use a wide variety of coupling agents, including 2,2,6,6-tetramethylpiperidinoxyl (TEMPO),[15] *N*-*tert*-butyl-1-diethylphosphono-2,2-dimethylpropylnitroxyl (DEPN),[5] β-phosphonated nitroxides,[10] di-*tert*-butyl nitroxide,[7] and others.[4,11,13]

The ability to carry out NM-CRP depends on the monomer used and its ability to form bonds with the nitroxide moiety that can be reversibly cleaved at reasonable temperatures. The NM-CRP of styrene has been the most widely studied.[6,7,9,12,14−16] The NM-CRP of styrene consists of the following four basic steps: (1) initiation, which occurs by chemical decomposition of initiator and thermal initiation; (2) propagation, where initiator and polymer radicals react with styrene monomer to produce growing polymer chains; (3) end-chain coupling, where radical chains are reversibly coupled with nitroxide radicals; and (4) termination, by recombination or disproportionation of radicals.

Several papers have addressed the mechanism and kinetics of "living" free radical polymerization,[6,8,9,12,14−16] and a detailed review of the literature may be found in the paper by Hawker et al.[17] While the importance of propagation, chain transfer to monomer, coupling, and termination is well established, the contributions of thermal initiation, chain transfer to polymer, and hydrogen transfer to the nitroxide radical are less clear. Literature reports have differed over their assessment of the impact of these additional reactions on the NM-CRP of styrene, where it has been reported that some of these reactions have a considerable effect on the kinetics of styrene polymerization[18−21] or only a slight impact.[12,22]

The contribution of thermal polymerization is considered to be small due to the belief that low polymerization temperatures suppress thermal initiation of styrene sufficiently.[12] Two mechanisms have been pro-

[†] Department of Chemical Engineering.
[‡] Department of Materials Science and Engineering.
* To whom correspondence should be addressed: Phone 847-491-5351; Fax 847-491-3728; e-mail broadbelt@northwestern.edu.

10.1021/ma030091v CCC: $25.00
Published on Web 09/04/2003

posed to explain self-initiated polymerization. The Flory mechanism[23] involves two styrene molecules forming a diradical, which after hydrogen abstraction becomes a monoradical and forms the initiator. The Mayo[24] mechanism involves three styrene molecules: two styrene molecules react to form reactive dimer, which in turn reacts with the third styrene molecule to form two initiating radicals to produce polystyrene chains. The Mayo mechanism has greater support based on kinetic investigations and isotope effect studies.[25] Only a few research groups have considered thermal initiation to be important, and they only considered it to be important at polymerization temperatures at or above 90 °C.[6,18] The influence of extra and self-initiation on NM-CRP has been treated theoretically by Souaille and Fischer,[26] where it was determined that the external or self-initiation rate should be kept below 1% of the initial rate of the decoupling reaction to maintain control over the polymerization.

A second step that is usually neglected is chain transfer to polymer, where end-chain radicals abstract hydrogen to form midchain radicals. The formation of midchain radicals leads to branching, and from literature data[27] it is apparent that branching during styrene polymerization occurs mainly from chain transfer to polymer. However, the amount of branching that occurs during styrene polymerization is believed to be very minor.[27] Quantitative parameters that govern the contribution of chain transfer to polymer have not been established during NM-CRP.

The role of hydrogen transfer from hydroxy amines to polymeric radicals has also been conjectured to affect the polymerization kinetics.[21,28,29] Polymeric and nitroxide radicals can react via disproportionation, forming an olefinic end group and a hydroxy amine. A polymeric radical can then abstract hydrogen from the hydroxy amine, effectively terminating a growing chain and regenerating the nitroxide radical. Depending on the magnitude of the decomposition rate constant, this reaction may cause a broadening of the polymer polydispersity, limiting the "living" nature of the polymerization. The identity of the nitroxide species and the propensity of the polymeric radicals to disproportionate are factors that would determine the importance of this reaction.

It is apparent that a complete understanding of "living", or controlled, free radical polymerization of styrene is still lacking. In particular, we sought to understand data collected in our laboratory[1] at different temperatures and using both a unimolecular initiator at different concentrations and a macroinitiator. Our approach to developing this understanding was to first create a detailed mechanistic model of NM-CRP that contained the basic steps mentioned above. However, developing a detailed mechanistic model required the specification of rate parameters, and the rate parameters for the coupling reaction were not available in the literature. After implementing an Evans−Polanyi[30] description of the activation energy into the model ($E = E_0 + \alpha\Delta H_R$) and using rate parameters from the literature and previous modeling work in our laboratory,[2,3] the model was fit to experimental data for the NM-CRP of styrene at 87 °C and with a specific initiator to obtain a fitted heat of reaction for the coupling reaction (ΔH_R) and an intrinsic barrier (E_0) for propagation/depropagation. The model was also fit with chain transfer to monomer, and both chain transfer to monomer and styrene thermal initiation were included in the model to determine the impact that these reactions have on the kinetics. The model with the best fit was then used to simulate the kinetics of a living styrene system at different temperatures and with a macroinitiator without further adjustment of the parameters. In addition, the importance of chain transfer to polymer and hydrogen transfer involving nitroxide radicals was assessed by incorporating these reactions into the model and observing changes in the model output. The model results were compared to experimental data collected for NM-CRP of styrene using α-methylstyryl (A)−di-*tert*-butyl nitroxide (T) ($C_6H_5CH(CH_3)-ONC(CH_3)_3C(CH_3)_3$, referred to as A−T) as a unimolecular initiator.

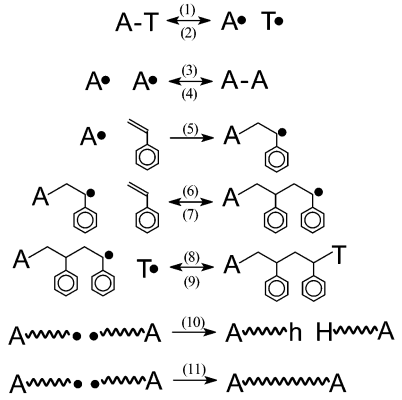

Figure 1. Reactions included into the base model for the NM-CRP of styrene. The reactions are numbered in the preceding text.

Model Development

Mechanistic Chemistry. The fundamental reactions governing the NM-CRP of styrene using the unimolecular initiator A−T are as follows: (1) initiation through bond fission of A−T, (2) initiator recombination, (3) recombination of A• radicals, (4) fission of A−A species, (5) addition of initiator to monomer, (6) propagation, (7) depropagation, (8) coupling with T• radicals, (9) T decoupling, (10) radical recombination, and (11) disproportionation. These reactions are illustrated in Figure 1. Initiation, which occurs by the chemical decomposition of initiator (in our case, A−T to radicals A• and T•), creates free radicals. The free radicals A• and T• or A• and A• were then allowed to recombine to form initiator or dead polymers respectively. These species were also allowed to subsequently undergo fission to reproduce the A• and T• radicals. The T• radical was assumed to not react with styrene, while the A• radical reacts with monomer via a radical addition step to facilitate the growth of a polymer chain. Propagation then continues with the addition of styrene to a growing polymer chain. The coupling reaction entails reversibly coupling growing polymeric chains with nitroxide radicals (T•). Finally, termination occurs by recombination or disproportionation of polymeric end-chain radicals. These basic reactions can be lumped into five typical free radical reaction families: bond fission, radical addition, β-scission, disproportionation, and radical recombination. Initiation and decoupling are bond fission reactions, addition of initiator to monomer and propagation are radical addition reactions, depropagation is an end-chain β-scission reaction, and termination of the radicals

A• and T• with themselves or with polymer radicals are radical recombinations. The T• radical was assumed to be stable, i.e., did not undergo any decay reactions, due to the slow rate of decay at the temperatures studied in this work based on half-life.[31]

A simple kinetic analysis can be carried out for these basic steps to probe the dependence of molecular weight on initiator concentration. In work performed by Gray et al.[1] (the companion paper to the modeling study), the assumptions that (1) the coupling reaction is in equilibrium and (2) the concentrations of the coupling agent and the coupled chains are described by the expressions derived by Fukuda et al.[32] were combined to obtain an expression for the concentration of polymeric radicals. Gray and co-workers then concluded from their expression that $DP_n \propto M_n \propto 1/C_0^{2/3}$, where DP_n is the degree of polymerization, M_n is the number-average molecular weight, and C_0 is the initial unimolecular initiator concentration. Hence, the number-average molecular weight is proportional to the initial concentration of A−T to the −2/3 power.

Gray and co-workers then quantitatively compared the main result of this simple kinetic analysis to experimental data where the initial concentration of initiator was varied. The study by Gray et al.[1] shows NM-CRP data collected at three different polymerization temperatures (77, 87, and 97 °C) for a wide range of initial initiator concentrations (0.000007−0.0131 mol/L). It is clear that their experimental data does not follow the dependence of M_n on $C_0^{-2/3}$ over the full range of A−T concentrations investigated, as the data only follows this linear dependence at high A−T initial concentrations. We therefore sought to explain this deviation by including the other proposed reactions. Using the fundamental reactions in Figure 1 as a base, side reactions of interest were considered by individually adding them to the model. Side reactions considered included chain transfer to monomer, the thermal initiation of styrene, hydroxy amine formation, and chain transfer to polymer. These reactions are illustrated in Figure 2. For chain transfer to monomer, the reactions added included chain transfer to form a monomeric radical (12) and the reaction of this monomeric radical with monomer (13) to start a new propagating chain. For styrene thermal initiation, the reactions added to the model included three styrene molecules reacting to form two radicals (14) and the reaction of these radicals with monomer in a propagation reaction (15) to start a new polymer chain (similar to the overall reaction associated with the Mayo thermal initiation mechanism discussed earlier). This thermal initiation mechanism implemented is identical to the mechanism used by Hui and Hamielec[33] in studies on obtaining rate parameters for the thermal initiation of styrene. For hydroxy amine formation, the reactions added included disproportionation of a T• radical with an end-chain radical to form the hydroxy amine (16) and then a hydrogen transfer reaction between the hydroxy amine and an end-chain radical (17). Last, for chain transfer to polymer the reactions added included chain transfer to form a midchain radical (18), midchain radical recombination (19), and propagation of styrene onto a midchain radical to start a growing branch (20). Because it was not possible to obtain a simple analytical expression with these added complexities, detailed kinetic modeling was carried out.

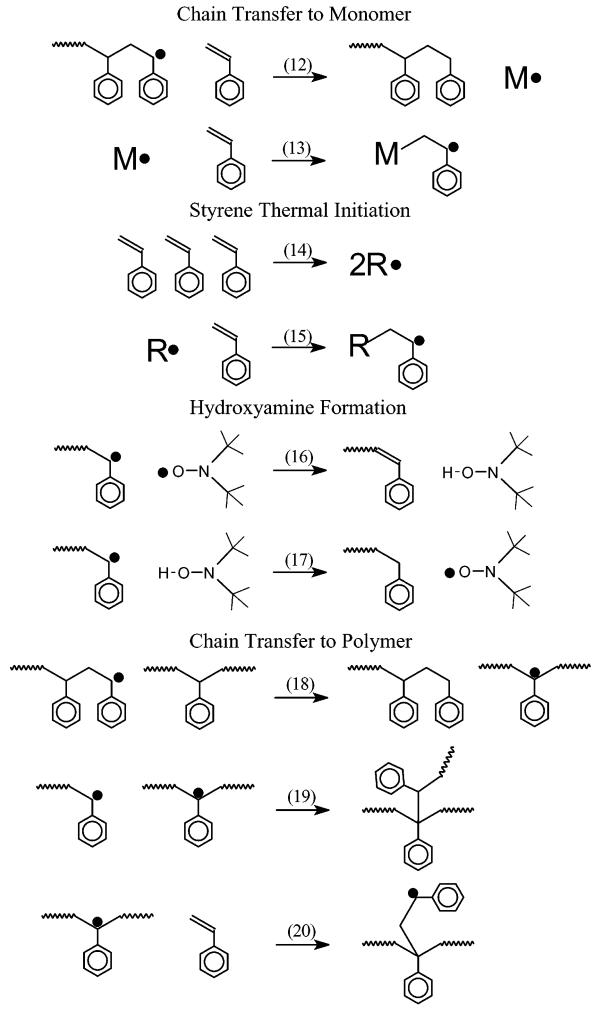

Figure 2. Side reactions incorporated into the model for styrene NM-CRP. The reactions are numbered in the preceding text, and the "h" and "H" chain ends represent saturated and unsaturated head ends, respectively.

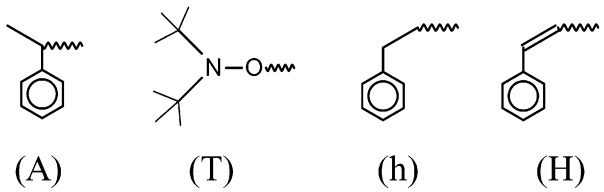

Figure 3. End-chain types tracked in the base model for the NM-CRP of styrene using the A−T initiator.

The method of moments was used to follow the growth of polymeric chains in the mechanistic model using population balance equations. The development of moment equations for propagation, depropagation, chain transfer, chain fission, and radical recombination has been covered extensively in the literature, and the moment equations used in our model are detailed elsewhere[3] and are summarized below. Briefly, polymeric species of interest were tracked by lumping polymer chains into groups, as done previously,[3] according to the location of the radical center and the end-chain structures. The end-chain structures tracked for the base model (model including only reactions in Figure 1) are shown with their labels in Figure 3, and from these four different end-chain groups, 10 possible nonradical linear chains can be developed. Four of the 10 nonradical polymer groups tracked are shown in Figure

1, which are polymer with an A and a T end (P_AT), polymer with an A and an h end (P_Ah), polymer with an A and an H end (P_AH), and polymer with two A ends (P_AA). Since all monomer was assumed to add to radicals such that the radical remained on the head end of a monomer unit due to the predominance of "head"-to-"tail" linkages in polystyrene,[34] polymer chains with tail ends (except for A ends) were never formed in the model. This method also allows different types of nonradical species and different types of end-chain radicals to be distinguished within the model, where, from the four ends tracked for the base model, four possible polymeric radicals could be formed (all four having a head end-chain radical). To facilitate model construction for all the models developed, programs were developed using the programming language Perl to assemble moment (zeroth, first, and second) equations from input of the polymeric features to be tracked. The set of differential equations was solved using DASSL.[35]

Moment Equations for Specific Chain Fission/ Radical Recombination. This chain fission involves the fission of a specific bond near the end of a polymer chain to form a low molecular weight radical, as shown in reaction 9 of Figure 1 for the decoupling reaction. This reaction can be represented generically as shown in reaction a in terms of polymer (P) and end-chain radicals (Re), where the subscripts denote the chain lengths in terms of the number of monomer units, k_{fs} is the rate constant for cleavage of the specific bond, and k_c is the rate constant for combination of radicals. The low molecular weight radical produced is represented by r_s, and s is the length of the low molecular weight radical in monomer units. Moment equations for this reaction have been developed by McCoy and co-workers[36,37] and are given in eqs 2 and 3. The low molecular weight radical concentration is monitored through eq 4. The superscripts denote the moments of the species.

$$\mathrm{P}_n \overset{k_{fs}}{\underset{k_c}{\longleftrightarrow}} \mathrm{Re}_{n-s} + \mathrm{r}_s \qquad \text{(a)}$$

$$\binom{m}{j} = \frac{m!}{j!(m-j)!} \qquad (1)$$

$$\frac{\mathrm{d}P^m}{\mathrm{d}t} = -k_{fs}\mathrm{P}^m + k_c\sum_{j=0}^{m}\binom{m}{j}\mathrm{Re}^{m-j}(s)^j[\mathrm{r}_s] \qquad (2)$$

$$\frac{\mathrm{dRe}^m}{\mathrm{d}t} = k_{fs}\sum_{j=0}^{m}\binom{m}{j}(-s)^j\mathrm{P}^{m-j} - k_c\mathrm{Re}^m[\mathrm{r}_s] \qquad (3)$$

$$\frac{\mathrm{d}[\mathrm{r}_s]}{\mathrm{d}t} = k_{fs}\mathrm{P}^0 - k_c\mathrm{Re}^0[\mathrm{r}_s] \qquad (4)$$

Moment Equations for Depropagation/Propagation. Depropagation (end-chain β-scission) and propagation are represented below in reaction b where M represents monomer produced, k_{dp} is the rate constant for depropagation, and k_p is the rate constant for propagation. The moment equations for this reaction are similar to those for specific chain fission. The moment equations for the end-chain radical are given in eq 5, and the monomer concentration is monitored using eq 6.

$$\mathrm{Re}_n \overset{k_{dp}}{\underset{k_p}{\longleftrightarrow}} \mathrm{Re}_{n-1} + \mathrm{M} \qquad \text{(b)}$$

$$\frac{\mathrm{dRe}^m}{\mathrm{d}t} = -k_{dp}\mathrm{Re}^m + k_p\sum_{j=0}^{m}\binom{m}{j}\mathrm{Re}^{m-j}[\mathrm{M}] + k_{dp}\sum_{j=0}^{m}\binom{m}{j}(-1)^j\mathrm{Re}^{m-j} - k_p\mathrm{Re}^m[\mathrm{M}] \qquad (5)$$

$$\frac{\mathrm{d}[\mathrm{M}]}{\mathrm{d}t} = k_{dp}\mathrm{Re}^0 - k_p\mathrm{Re}^0[\mathrm{M}] \qquad (6)$$

Moment Equations for Radical Recombination. Chain fission and radical recombination can be represented as shown in reaction c. Note that this reaction involves the combination of two polymeric radicals; in contrast, reaction a involved recombination of a polymeric radical and a specific small radical. Moment equations have been developed for this reaction[36,38,39] and are given in eqs 7 and 8.

$$\mathrm{Re}_i + \mathrm{Re}_{n-i} \xrightarrow{k_c} \mathrm{P}_n \qquad \text{(c)}$$

$$\frac{\mathrm{dP}^m}{\mathrm{d}t} = +\frac{1}{2}k_c\sum_{j=0}^{m}\binom{m}{j}\mathrm{Re}^j\,\mathrm{Re}^{m-j} \qquad (7)$$

$$\frac{\mathrm{dRe}^m}{\mathrm{d}t} = -k_c\mathrm{Re}^m\mathrm{Re}^0 \qquad (8)$$

Moment Equations for Disproportionation. Disproportionation involves the termination of two end-chain radicals to form two nonradical polymer species. This reaction is represented below in reaction d. Employing the method of moments, generation and consumption terms can be formulated for the polymer produced and the consumption of end-chain radicals as shown in eqs 9 and 10, respectively.

$$\mathrm{Re}_n + \mathrm{Re}_i \xrightarrow{k_d} \mathrm{P}_n + \mathrm{P}_i \qquad \text{(d)}$$

$$\frac{\mathrm{dP}^m}{\mathrm{d}t} = k_d\mathrm{Re}^m\mathrm{Re}^0 + k_d\mathrm{Re}^0\mathrm{Re}^m \qquad (9)$$

$$\frac{\mathrm{dRe}^m}{\mathrm{d}t} = -k_d\mathrm{Re}^m\mathrm{Re}^0 - k_d\mathrm{Re}^0\mathrm{Re}^m \qquad (10)$$

Moment Equations for Hydrogen Abstraction. Hydrogen abstraction involves the abstraction of a hydrogen along the backbone of a polymer chain by an end-chain radical to produce a tertiary midchain radical. This reaction is illustrated as reaction 18 in Figure 2. Hydrogen abstraction is represented by reaction e where the Rm label represents the midchain radical produced. The moment expressions in eqs 11−13 are an extension of the expressions for chain transfer developed by Pladis and Kiparissides.[40] The variable N_H^m represents the number of abstractable hydrogen atoms per monomer unit in the middle of the chains. The e_t variable represents the number of monomer units along a polymer chain that do not undergo this general midchain hydrogen abstraction reaction (such as hydrogen on unsaturated units and chain-end units). Equation 14

Table 1. Representative Values of Kinetic and Thermodynamic Parameters for Reaction Types Incorporated into Base Mechanistic Model of Styrene NM-CRP (All Rate Parameters without Footnotes Were Obtained from Previous Modeling Work in our Laboratory,[2,3] and All Heats of Reaction without Footnotes Were Obtained from the NIST Database[44])

reaction type	frequency factor, A (s^{-1} or L mol^{-1} s^{-1})	intrinsic barrier, E_0 (kcal mol^{-1})	α, transfer coefficient	representative heat of reaction (kcal mol^{-1})	activation energy (kcal mol^{-1})
initiator decomposition	2.2×10^{14} [a]	2.3[d]	1.0	*24.2*,[h] *23.4*,[i] *22.7*[j]	*26.5*,[h] *25.7*,[i] *25.0*[j]
initiator recombination	4.7×10^{9} [b]	2.3[d]	0.0	*24.2*,[h] *23.4*,[i] *22.7*[j]	2.3
A−A decomposition	1.0×10^{16}	2.3[d]	1.0	64.0	66.6
initiator propagation	1.5×10^{7} [f]	*10.9*,[h] *11.1*,[i] *10.8*[j]	0.24	−24.8	*4.9*,[h] *5.1*,[i] *4.8*[j]
propagation	1.5×10^{7} [f]	*10.9*,[h] *11.1*,[i] *10.8*[j]	0.24	−17.5	*6.7*,[h] *6.9*,[i] *6.6*[j]
depropagation	4.1×10^{12} [g]	*10.9*,[h] *11.1*,[i] *10.8*[j]	0.76	17.5	*24.2*,[h] *24.4*,[i] *24.1*[j]
T coupling	4.7×10^{9} [b]	2.3[d]	0.0	*24.2*,[h] *23.4*,[i] *22.7*[j]	2.3
T decoupling	2.2×10^{14} [a]	2.3[d]	1.0	*24.2*,[h] *23.4*,[i] *22.7*[j]	*26.5*,[h] *25.7*,[i] *25.0*[j]
radical recombination	9.3×10^{10} [c]	2.3[d]	0.0	NA	2.3
disproportionation	1.7×10^{10} [e]	2.3[d]	0.0	NA	2.3

[a] Frequency factor for decoupling reaction obtained from Marque et al.[31] [b] Frequency factor for coupling reaction obtained from coupling rate constant of 2.5×10^{8} L/(mol s) at 120 °C for similar nitroxide radical.[48] [c] Termination frequency factor from data on the termination of 1-ethyl-2-phenyl radicals.[49] [d] Intrinsic barrier determined from polystyrene termination rate constants.[50] [e] Disproportionation estimated to be 15% of termination rate from Schreck et al.[51] [f] Frequency factor from Deady et al.[46] [g] Frequency factor backed out from equilibrium data.[34] [h] Fitted parameters for the base model. [i] Fitted parameters once chain transfer to monomer was included. [j] Fitted parameters once styrene thermal polymerization was included.

is the Saidel−Katz approximation for the third moment,[41] which is needed to obtain closure on the differential equations for the moments of nonradical polymeric species. Moment equations similar to these were developed for the abstraction of hydrogen from monomer during chain transfer to monomer.

$$\mathrm{Re}_n + \mathrm{P}_i \xrightarrow{k_{\mathrm{tr,e}}} \mathrm{P}_n + \mathrm{Rm}_i \qquad \text{(e)}$$

$$\frac{\mathrm{d}\mathrm{P}^m}{\mathrm{d}t} = -N_{\mathrm{H}}^m k_{\mathrm{tr,e}} \mathrm{Re}^0 (\mathrm{P}^{m+1} - e_{\mathrm{t}} \mathrm{P}^m) + N_{\mathrm{H}}^m k_{\mathrm{tr,e}} \mathrm{Re}^m (\mathrm{P}^1 - e_{\mathrm{t}} \mathrm{P}^0) \qquad (11)$$

$$\frac{\mathrm{d}\mathrm{Re}^m}{\mathrm{d}t} = -N_{\mathrm{H}}^m k_{\mathrm{tr,e}} \mathrm{Re}^m (\mathrm{P}^1 - e_{\mathrm{t}} \mathrm{P}^0) \qquad (12)$$

$$\frac{\mathrm{d}\mathrm{Rm}^m}{\mathrm{d}t} = N_{\mathrm{H}}^m k_{\mathrm{tr,e}} \mathrm{Re}^0 (\mathrm{P}^{m+1} - e_{\mathrm{t}} \mathrm{P}^m) \qquad (13)$$

$$\mathrm{P}^3 = \frac{2\mathrm{P}^2\mathrm{P}^2}{\mathrm{P}^1} - \frac{\mathrm{P}^2\mathrm{P}^1}{\mathrm{P}^0} \qquad (14)$$

Specification of Rate Constants. Once the moment equations were assembled, it was necessary to specify the kinetic parameters for each elementary step reaction included in the styrene NM-CRP model. Assuming the validity of the Arrhenius relationship, a frequency factor and an activation energy for each reaction were specified. It has been shown that coupling between some nitroxides and carbon-centered radicals does not follow the Arrhenius form, but for the T• used here, Arrhenius behavior is observed.[52] Each reaction of a given reaction family (e.g., bond fission) shared the same frequency factor. The activation energy for each specific reaction was calculated using the Evans−Polanyi relationship,[30] in which the activation energy is related linearly to the heat of reaction, i.e., $E = E_0 + \alpha \Delta H_{\mathrm{R}}$. Most of the values of the heats of reaction were obtained from experimental polymerization data or based on analogous reactions of molecular mimics of the polymer structure as used previously.[42−44] The frequency factors and the parameters E_0 and α for each reaction type were primarily obtained from the literature or previous modeling work in our laboratory,[2] and this approach was successfully used in our previous work to model the depolymerization of polystyrene.[3]

However, although the decoupling/coupling reactions are lumped into the bond fission/radical recombination reaction family, an exact heat of reaction for decoupling/coupling involving our particular T is not available in the literature. The model results were found to be extremely sensitive to this heat of reaction (which is used in the calculation of the activation energy using the Evans−Polanyi relationship), and thus an estimate of the heat of reaction from analogous nitroxide species was insufficient. Because of this high sensitivity, the model was fit to a set of experimental data reported in Gray et al.[1] for the NM-CRP of styrene at 87 °C to obtain the heat of reaction for coupling. These data at 87 °C were collected for a wide range of initial initiator concentrations (0.000007−0.0131 mol/L) and for polymerization times of 3.0 and 6.5 h.[1] In addition to fitting the heat of reaction for the coupling reaction, the intrinsic barrier, E_0, for radical addition was fit at the same time. The model results were also found to be extremely sensitive to this parameter, and because of slight discrepancies in the literature of the exact activation energy for radical addition (propagation), this value was also fit to see if a fitted value in agreement with values in the literature was obtained. The fitting was performed using GREG (*g*eneralized *reg*ression).[45]

The rate constants for propagation and termination were assumed to be independent of the chain length of the species involved due to the low styrene conversions in NM-CRP experiments. For the inclusion of chain transfer to polymer, the chain transfer frequency factor was assumed to be inversely proportional to the size of the polymer radical performing the hydrogen abstraction.[3] A method to track branching that was used previously[3] was implemented when chain transfer to polymer was included in the model. This method involved lumping all branched species into one group and then tracking the moments of this consolidated branched group. Table 1 summarizes the kinetic parameters used in the NM-CRP base model (parameters which were fit are italicized), and Table 2 gives the rate parameters used to describe the kinetics of the side reactions considered.

Results and Discussion

Model Fitting. As a baseline for comparison, a detailed kinetic model was developed for the core mechanism, i.e., the one which formed the basis for the simple kinetic analysis described in Gray et al.[1] (reac-

Table 2. Representative Values of Kinetic and Thermodynamic Parameters for Additional Reaction Types Incorporated into Mechanistic Model of Styrene NM-CRP (All Rate Parameters without Footnotes Were Obtained from Previous Modeling Work in our Laboratory,[2,3] and All Heats of Reaction without Footnotes Were Obtained from the NIST Database[44])

reaction type	frequency factor, A (s^{-1} or L mol^{-1} s^{-1})	intrinsic barrier, E_0 (kcal mol^{-1})	α, transfer coefficient	representative heat of reaction (kcal mol^{-1})	activation energy (kcal mol^{-1})
styrene thermal initiation	2.2×10^5 [e]	27.44[e]	NA	NA	27.44
initiator propagation	1.5×10^7 [d]	*10.9*,[h] *11.1*,[i] *10.8*[j]	0.24	−24.8	*4.9*,[h] *5.1*,[i] *4.8*[j]
hydroxy amine formation	1.0×10^4 [g]	NA	NA	NA	NA
hydroxy amine transfer	70.0[c]	NA	NA	NA	NA
chain transfer to polymer	2.1×10^6 [f]	12.0[f]	0.48	−3.1	10.5
chain transfer to monomer	2.3×10^6 [e]	12.7[e]	NA	NA	12.7
midchain radical recombination	9.3×10^{10} [a]	2.3[b]	0.0	NA	2.3
midchain propagation	1.5×10^7 [d]	*10.9*,[h] *11.1*,[i] *10.8*[j]	0.24	−14.4	*7.4*,[h] *7.6*,[i] *7.3*[j]

[a] Termination frequency factor from data on the termination of 1-ethyl-2-phenyl radicals.[49] [b] Intrinsic barrier determined from polystyrene termination rate constants.[50] [c] Rate constant from data obtained by He et al. at 90 °C;[21] no temperature dependence was given. [d] Frequency factor and intrinsic barrier from Deady et al.[46] [e] Rate parameters from Hui and Hamielec.[33] [f] Rate parameters from previous modeling work on polystyrene degradation.[3] [g] Rate constant estimated using coupling equilibrium constant at 90 °C.[18] [h] Fitted parameters for the base model. [i] Fitted parameters once chain transfer to monomer was included. [j] Fitted parameters once styrene thermal polymerization was included.

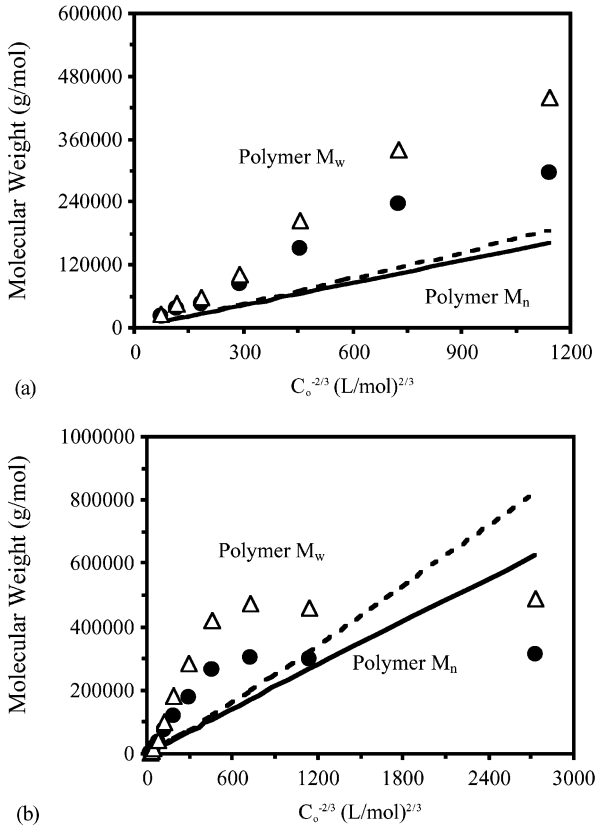

Figure 4. Comparison of the fitted model results for the base model to the experimental styrene NM-CRP data at 87 °C after (a) 3.0 h and (b) 6.5 h of polymerization. The heat of reaction for the decoupling reaction and the E_0 for propagation/depropagation were the fitted parameters.

tions in Figure 1). This model was fit to experimental data from Gray and co-workers at 87 °C where experimental data for styrene NM-CRP were collected for initial A−T concentrations between 0.000007 and 0.0131 mol/L and for polymerization times of 3.0 and 6.5 h.[1] The results of the model fitting are shown in Figure 4. The values of the fitted parameters obtained were E_0 for propagation/depropagation = 10.92 ± 0.88 kcal/mol and ΔH_R for the T decoupling reaction = 24.20 ± 2.31 kcal/mol. As is illustrated by Figure 4, the fitted model results are in poor agreement with the experimental data after 3.0 and 6.5 h of polymerization. The model predicted the expected linear dependence of M_n vs $C_0^{-2/3}$ over the full range of concentrations studied, but the experimental data deviate from this trend at low initial A−T concentrations. Both the number- and weight-average molecular weights for the model results deviate quite significantly from the experimental values in the region where the experimental M_n and M_w values bend over while the model remains linear.

The first step in assessing what phenomenon was responsible for the nonlinear behavior of the experimental data was to include chain transfer to monomer into the model and then perform a fit of the model again to all of the experimental data at 87 °C. Chain transfer to monomer is normally considered to be a fundamental part of the styrene polymerization mechanism, but adding it incrementally to the base mechanism and performing the fitting once again allowed its contribution to the bend in the experimental data to be isolated. For this expanded model, the reactions shown in Figure 2 for chain transfer to monomer and all of the reactions in Figure 1 were incorporated into the model. The expanded model tracked five types of end-chain structures (A, T, h, H, and M ends). The intrinsic kinetic parameters governing chain transfer to monomer are reported in Table 2. The results of this model fitting are shown in Figure 5, and the values of the fitted parameters obtained were E_0 for propagation/depropagation = 11.10 ± 0.43 kcal/mol and ΔH_R for the T decoupling reaction = 23.35 ± 1.12 kcal/mol. These fitted parameters are slightly different from the fitted parameters obtained for the base model, indicating chain transfer to monomer has an impact on the kinetics. However, similar to the base model, the model predicted a close to linear dependence of M_n on $C_0^{-2/3}$ over the full range of initiator concentrations studied. Both the number- and weight-average molecular weights predicted by the model deviated quite significantly from the experimental values. This expanded model was unable to predict the bend in the M_n and M_w data at low initiator concentrations.

The second step in assessing what phenomenon was responsible for the nonlinear behavior was to include thermal initiation into the model and then perform a fit of the model again to all of the experimental data at 87 °C. For this model, the reactions shown in Figure 2 for styrene thermal initiation and chain transfer to monomer and all of the reactions in Figure 1 were incorporated into the model. Within this expanded model, six types of end-chain structures were tracked

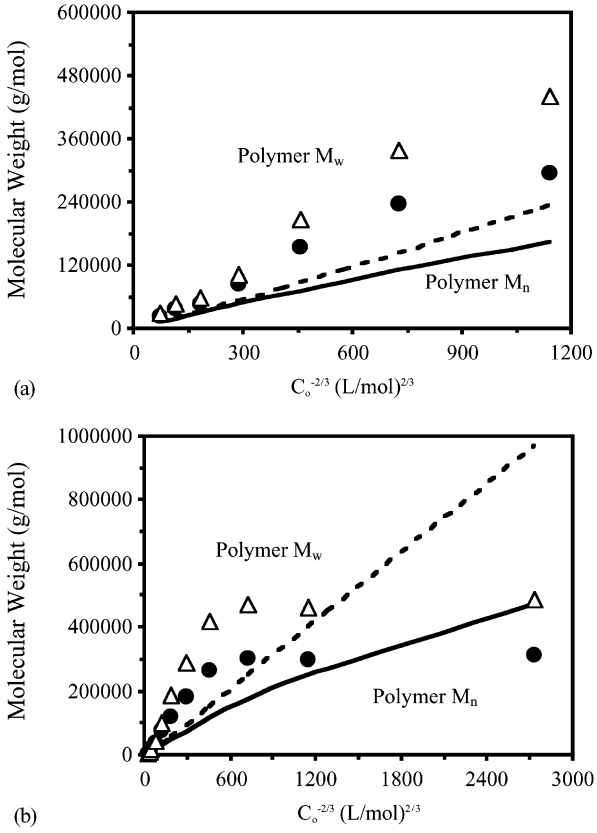

Figure 5. Comparison of the fitted model results for the model including chain transfer to monomer to the experimental styrene NM-CRP data at 87 °C after (a) 3.0 h and (b) 6.5 h of polymerization. The heat of reaction for the decoupling reaction and the E_0 for propagation/depropagation were the fitted parameters.

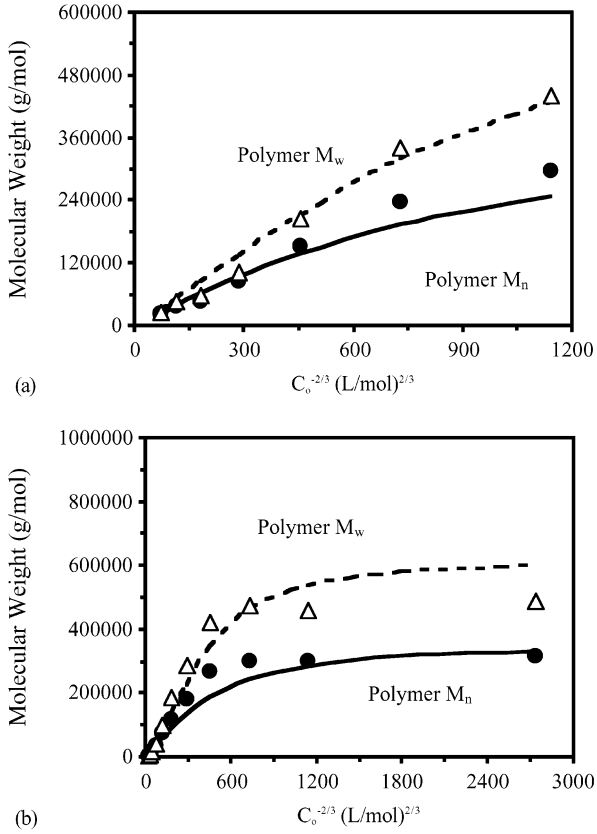

Figure 6. Comparison of the fitted model results for the model including styrene thermal initiation and chain transfer to monomer to the experimental styrene NM-CRP data at 87 °C after (a) 3.0 h and (b) 6.5 h of polymerization. The heat of reaction for the decoupling reaction and the E_0 for propagation/depropagation were the fitted parameters.

(A, T, h, H, M, and R ends). The intrinsic kinetic parameters governing the thermal initiation of styrene are reported in Table 2. The results of this model fitting are shown in Figure 6, and the values of the fitted parameters obtained were E_0 for propagation/depropagation = 10.78 ± 0.08 kcal/mol and ΔH_R for the T decoupling reaction = 22.70 ± 0.40 kcal/mol. The fitted intrinsic barrier for propagation/depropagation gives an activation energy for propagation of 6.6 kcal/mol that is similar to the propagation activation energies reported in the literature (~7.0 kcal/mol).[46,47] However, our fitted intrinsic barrier is likely a little low since the chain length dependence for polymer−polymer termination is neglected in the model, and even at low polymer concentrations a small termination chain length dependence has been observed.[34] The fitted ΔH_R for the decoupling reaction is also in agreement with data in the literature, where ΔH_R for the decoupling reaction involving the TEMPO nitroxide radical was estimated to be 22.0 kcal/mol.[15] The results of fitting the experimental data to this model are considerably better than when thermal initiation was neglected. The experimental and model results are in very good agreement after both 3.0 and 6.5 h of polymerization. The deviation from linearity at low A−T concentrations is nicely captured after 6.5 h of polymerization when thermal initiation is included. The only minor disagreement between the model results and the experimental data is the higher PDI values obtained from the model at low initiator concentrations. These model results indicate that thermal initiation cannot be ignored even at temperatures as low as 87 °C.

To probe why including the thermal initiation of styrene is critical to obtaining the correct behavior within the model, an analysis of the relative fractions of the types of live and dead chains within the fitted model results for the base model and the model including styrene thermal initiation was performed. Figures 7 and 8 show the fractions of the live and dead chains within the model results for three different initial A−T concentrations for the base model and the model with styrene thermal initiation included, respectively. As is evident from Figure 7, at low A−T concentrations a significant fraction of the living chains are terminated during the course of the polymerization. However, the base model predicts that the majority of the polymer chains remain alive even at low A−T concentrations, and thus the polymerization behaves as expected for NM-CRP. A polymer with narrow polydispersity is produced according to the base model at all initiator concentrations, and the molecular weight follows the dependence on initiator concentration expected from the simple kinetic analysis.

A very different phenomenon appears to be occurring with the model including styrene thermal initiation as depicted in Figure 8, where nearly all of the chains are terminated at low A−T concentrations after a couple of hours. The major difference for the model including thermal initiation is that the chains that are still living after 1 h of polymerization at low A−T concentrations have all been initiated via thermal initiation (chains labeled P_RT). Unlike the chains initiated by A$^\bullet$ radicals, which are all initiated at the beginning of the

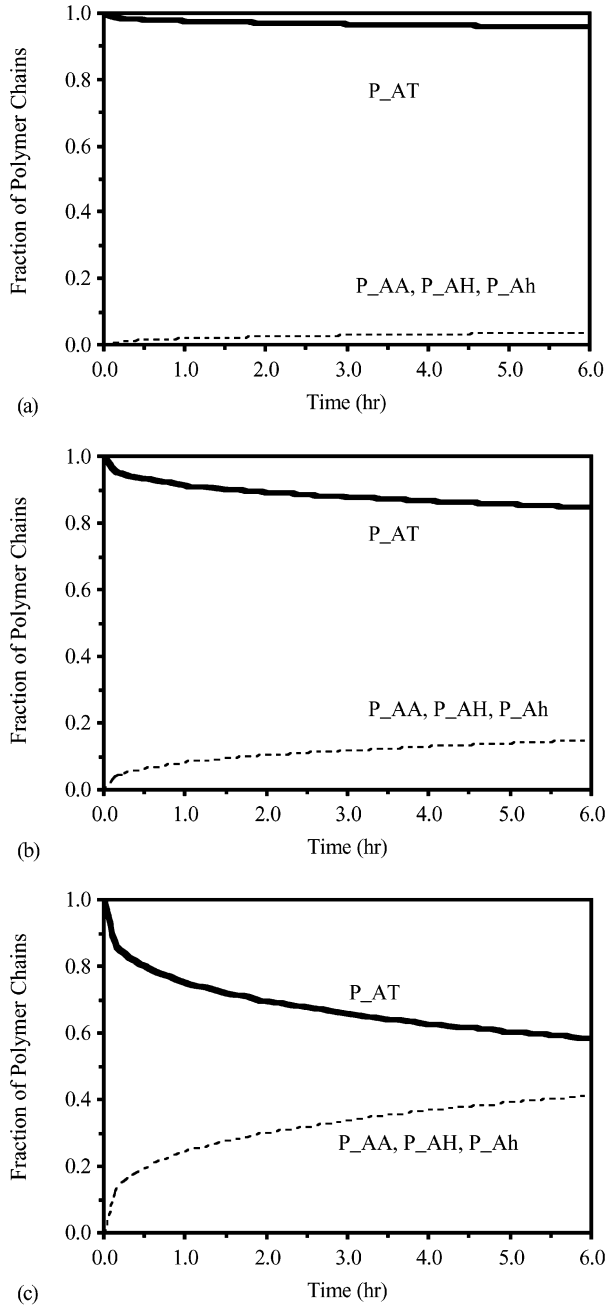

Figure 7. Fraction of living and terminated chains for base model runs with initial initiator concentrations of (a) 0.0131, (b) 0.000205, and (c) 0.000007 mol/L.

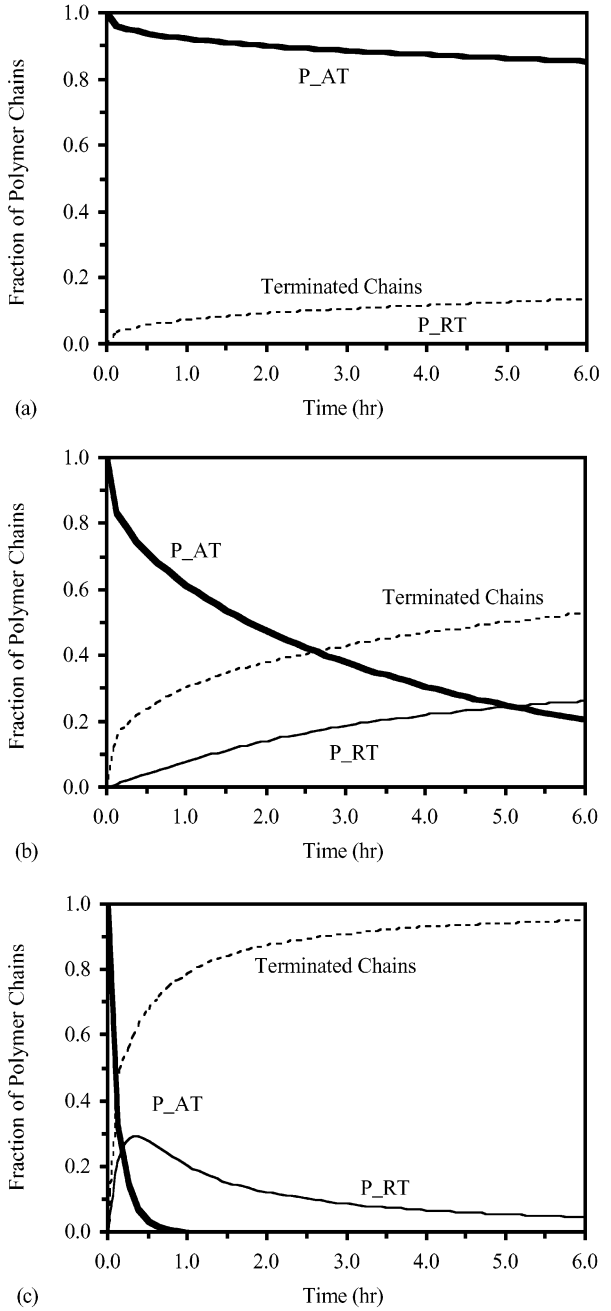

Figure 8. Fraction of living and terminated chains for runs with the model including styrene thermal initiation and chain transfer to monomer with initial initiator concentrations of (a) 0.0131, (b) 0.000205, and (c) 0.000007 mol/L.

polymerization process, these chains are being initiated at a relatively constant rate during the course of the polymerization. Thus, in contrast to the P_AT fraction, the P_RT fraction is not a high molecular weight, growing fraction that has been alive since the beginning of the polymerization process. Instead, it consists of chains of relatively constant molecular weight where chains that leave the group via termination are replaced by new thermally initiated chains (similar to what occurs during conventional free radical polymerization, except here the lifetime of each chain is much longer). Below a certain A−T concentration, the majority of the initiation is occurring via styrene thermal initiation, and the molecular weight of the final polymer product is independent of the initial A−T concentration.

Model Predictions. The fitted rate parameters for the model including styrene thermal initiation were then tested by using them without any further adjustment to predict the M_n and M_w at different temperatures and using a macroinitiator. The model results for the NM-CRP of styrene at 77 and 97 °C are compared to experimental data from Gray and co-workers[1] after 6.5 h of polymerization in Figure 9. The model results are also compared to experimental data obtained using a macroinitiator with an initial M_n equal to 18 200 g/mol at 87 °C. The macroinitiator was composed of a polystyryl radical coupled with di-*tert*-butyl nitroxide. The model was able to capture the M_n and M_w data at 77 and 97 °C fairly well. In addition, the behavior of the system with a macroinitiator was modeled accurately.

To examine the model predictions further, Figure 10 compares the model results for the NM-CRP at 87 and 97 °C. The model was able to accurately predict a

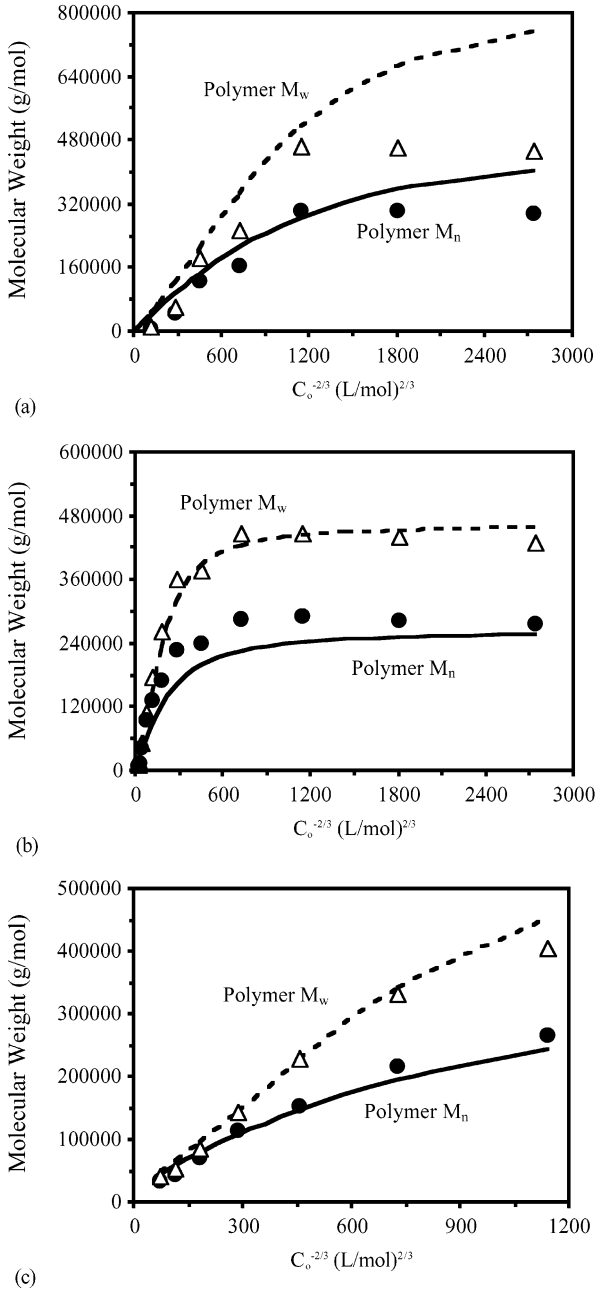

Figure 9. Comparison of the model results for the model including styrene thermal initiation and chain transfer to monomer to experimental data for styrene NM-CRP at (a) 77 °C after 6.5 h, (b) 97 °C after 6.5 h, and (c) 87 °C after 3.0 h, where for the 87 °C data a macroinitiator was used.

crossover point in the experimental M_n and M_w data at 87 and 97 °C. At high A−T concentrations the molecular weight of the polymer product is greater at the higher temperature, which is expected during a "living" polymerization. However, during normal free radical polymerization, at higher temperatures a polymer product with a lower molecular weight is produced. The model is able to predict a crossover point where the NM-CRP using the A−T initiator transitions to a state where the polymerization behaves as if it is conventional free radical polymerization. In Figure 10, it is noted that above an initial initiator concentration of 0.00008 mol/L NM-CRP seems to dominate, while below this concentration the polymerization is dominated by thermal initiation and the molecular weight development behaves like conventional free radical polymerization.

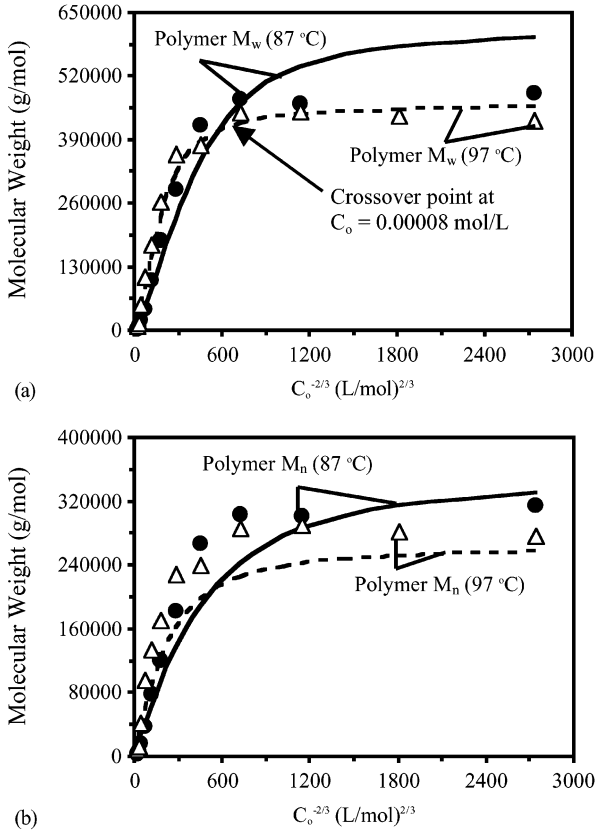

Figure 10. Comparison of model and experimental results for styrene NM-CRP at 87 °C after 6.5 h of polymerization for (a) M_w and (b) M_n. A crossover in the M_n and M_w data was observed in the experiments and is predicted by the model.

To examine this transition region between NM-CRP and free radical polymerization, these results were compared to the results obtained by Souaille and Fischer, in which they examined the extent to which self-initiation leads to a loss of control over nitroxide-mediated polymerization.[26] They determined that the external or self-initiation rate must remain below 1% of the initial cleavage rate of the coupling agent. According to Souaille and Fischer, the value of 1% should be viewed as an upper limit for controlled radical polymerizations in general; above this limit all control over any polymerization will be lost. This suggests that for some systems the external or self-initiation rate may need to be kept well below 1% to maintain control. Using the rate parameters in Tables 1 and 2, we calculated that the styrene thermal initiation rate is about 0.04% of the initial fission rate at $C_0 = 0.00008$ mol/L, and the styrene thermal initiation rate was always at or below 0.5% (0.5% for $C_0 = 0.000007$ mol/L) of the initial fission rate. For the NM-CRP system examined in this work, the self-initiation rate needs to be kept well below 1% of the initial cleavage rate of the coupling agent to maintain control over the polymerization.

To obtain a better understanding of why thermal initiation disrupts the NM-CRP of styrene, the initiator concentration at which control of the polymerization was lost is examined further in Figure 11. In Figure 11, the PDI values of the experimental results after 6.5 h are compared to the fraction of the total initiating radicals that were produced from styrene thermal initiation (F_{th}) after 6.5 h of NM-CRP. The quantity of initiating radicals produced from styrene thermal initiation was determined from the model results, where the rate of

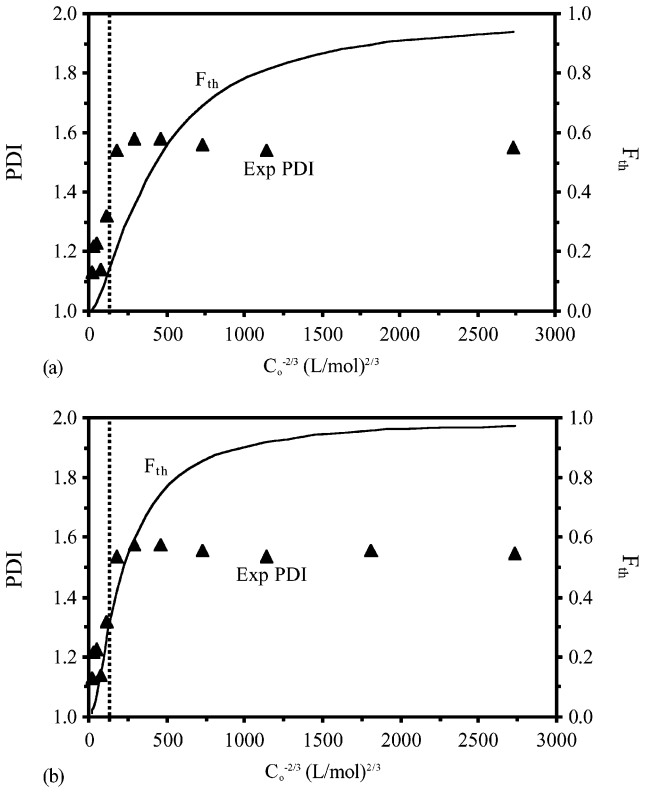

Figure 11. Comparison of experimental PDI results for styrene NM-CRP at (a) 87 °C and (b) 97 °C to the fraction of initiating radicals produced from styrene thermal initiation (F_{th}) predicted from the model results after 6.5 h of polymerization. The vertical dotted lines divide the PDI results between regions where LFRP dominates (left of dotted lines) and free radical polymerization dominates (right of dotted lines).

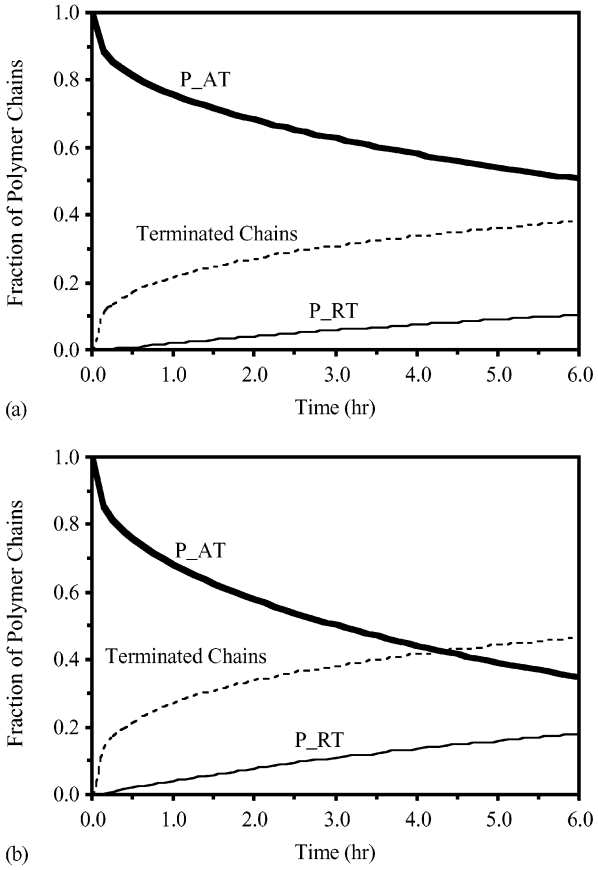

Figure 12. Fraction of living and terminated chains for runs with the model including styrene thermal initiation and chain transfer to monomer with initial initiator concentrations of (a) 0.00082 and (b) 0.00041 mol/L.

styrene thermal initiation was integrated from 0 to 6.5 h. The quantity of initiating radicals produced from the degradation of the unimolecular initiator (A•) was set equal to the initial concentration of A−T since all of the A−T degrades in the first minute of the polymerization to produce A• and T• radicals. As can be seen from Figure 11a,b, control over the polymerization, as measured by an increase in the PDI value above 1.5, is lost when more than 20−30% of the initiating radicals were produced from styrene thermal initiation (>20% for 87 °C and >30% for 97 °C). This alternative view of the experimental results indicates that control over the polymerization was lost at an even higher C_0 value than that indicated by the crossover point in Figure 10; below a C_0 value of 0.00082 mol/L at 87 °C the PDI after 6.5 h was greater than 1.5. The vertical dotted lines in Figure 11a,b separate the regions where NM-CRP is controlling the molecular weight development (to the left of the dotted lines) from the regions where free radical polymerization is the dominant polymerization mechanism (to the right of the dotted lines).

The analysis of the fractions of living and terminated chains for initial initiator concentrations of 0.00082 and 0.00041 mol/L shown in Figure 12 provides some insight into why control over the polymerization is lost when a small percentage of the initiating radicals has been produced from self-initiation. The C_0 values of 0.00082 and 0.00041 mol/L represent the experimental data points just to the left and just to the right of the dotted line in Figure 11a, respectively. For a C_0 value of 0.00082 mol/L, 12% of the initiating radicals were produced from styrene thermal initiation at 87 °C after 6.5 h of polymerization. For a C_0 value of 0.00041 mol/L, 21% of the initiating radicals were produced from styrene thermal initiation at 87 °C after 6.5 h of polymerization. As is evident from Figure 12a, the largest fraction of polymer chains after 6.5 h for a C_0 value of 0.00082 mol/L is living chains initiated by A• radicals, which is expected for the NM-CRP of styrene. In contrast, the largest fraction of polymer chains after 6.5 h for a C_0 value of 0.000 41 mol/L is terminated chains, as shown by Figure 12b. This indicates that the creation of a surplus of initiating radicals compared to the quantity of the coupling agent due to styrene self-initiation has led to a significant degree of termination between decoupled chains. In addition, after 6.5 h for a C_0 value of 0.000 41 mol/L the fraction of living chains initiated from radicals produced from styrene self-initiation (P_RT) has increased considerably compared to a C_0 value of 0.00082 mol/L. This group of living chains is not a growing fraction that has been alive since the start of the polymerization, but is instead a group of living chains that started their growth at different times during the polymerization process. Thus, this fraction of living chains is very polydisperse. With the population of terminated chains being the dominant type of polymer chains and the population of polymer chains initiated by styrene thermal initiation becoming very significant, the PDI is above 1.5 for the entire polystyrene mixture after 6.5 h for a C_0 value of 0.00041 mol/L. To maintain control over the polymerization process, living polymer chains initiated from the unimolecular initiator (P_AT) must remain the largest

fraction of polymer chains. This was only accomplished in our system if the percent of initiating radicals produced from self-initiation remained below 20−30%.

Effects of Side Reactions. The next possible side reaction examined in NM-CRP was the formation of a hydroxy amine. This involves a disproportionation reaction between nitroxide radicals and polymeric radicals to give the corresponding hydroxy amine by hydrogen transfer and polymer with an unsaturated end-chain group (as shown in Figure 2). Further, the hydroxy amine can then react with polymeric radicals, regenerating the nitroxide radical and terminating the polymer chain as a saturated chain. Using values for the associated rate constants from the literature as summarized in Table 2, it was found that the reaction does not affect the polymerization kinetics significantly. Including these reactions led to slightly higher polydispersity values at high initiator concentrations, but the values increased by less than 1%. This demonstrates that although this reaction is feasible, it is not significant at the NM-CRP conditions studied in this investigation.

The next side reaction investigated was chain transfer to polymer. The rate constants used to model this reaction were from previous modeling work performed in our laboratory (see Table 2), and the branching reactions that can occur upon formation of midchain radicals are shown in Figure 2. The dependence of M_n and M_w on the initial concentration of initiator (A−T) was found to be slightly affected when chain transfer to polymer was included. The only effect was a slight increase in the polydispersity values at a temperature of 97 °C for the lowest initial initiator concentrations, but the values increased by less than 3%.

Conclusions

The controlled free radical nitroxide-mediated bulk polymerization of styrene was modeled at the mechanistic level using the method of moments. The mechanistic models developed described the kinetics and the molecular weight development of the living free radical polymerization process. A base model was constructed which included initiator decomposition, propagation, end-chain coupling, and termination by recombination and disproportionation. The base model was fit to a set of experimental data for the NM-CRP of styrene at 87 °C to obtain a heat of reaction for coupling (ΔH_R for di-*tert*-butyl nitroxide coupling agent) and a fitted intrinsic barrier for propagation/depropagation. The rest of the rate parameters were obtained from the literature. This fit was then compared to the fit obtained when chain transfer to monomer and both chain transfer to monomer and styrene thermal initiation were included in the mechanism. It was found that including styrene thermal initiation was critical to being able to fit the mechanistic model to the experimental data. The fitted parameters obtained were E_0 for propagation/depropagation = 10.78 ± 0.08 kcal/mol and ΔH_R for the decoupling reaction = 22.70 ± 0.40 kcal/mol. Using these fitted parameters, the ability of the model to predict the evolution of M_n and M_w over a 20 °C temperature range and for different initial concentrations of initiator and macroinitiator was shown. The importance of reactions such as chain transfer to polymer and the reaction between a nitroxide radical and a polymeric radical to form a hydroxy amine was also investigated, and it was found that these reactions were negligible.

Acknowledgment. This work was supported by the MRSEC program of the National Science Foundation (DMR-0076097) at the Materials Research Center of Northwestern University and the CAREER Program of the National Science Foundation (CTS-9623741). Funding was also provided through a National Science Foundation Fellowship (Todd M. Kruse) and an IMGIP Fellowship (Maisha K. Gray).

Nomenclature

A = frequency factor, s^{-1} or L/(mol s)
C_0 = initial concentration of unimolecular initiator, mol/L
DP_n = degree of polymerization
e_t = number of monomer units without abstractable midchain hydrogen atoms
E = activation energy, kcal/mol
E_0 = intrinsic barrier, kcal/mol
F_{th} = fraction of initiating radicals produced from styrene thermal initiation
ΔH_R = heat of reaction, kcal/mol
i = chain length in number of monomer units
j = the jth moment of a species
k_c = radical recombination rate constant, L/(mol s)
k_d = disproportionation rate constant, L/(mol s)
k_{dp} = depropagation rate constant (end-chain β-scission), s^{-1}
k_{fs} = rate constant for fission at a specific location along a polymer chain, s^{-1}
k_p = propagation rate constant, L/(mol s)
$k_{tr,e}$ = chain transfer rate constant for the formation of a midchain radical from an end-chain radical, L/(mol s)
m = the mth moment of a species
M_n = number-average molecular weight, g/mol
M_w = weight-average molecular weight, g/mol
n = chain length in monomer units or number of branches
N_H^m = number of midchain abstractable hydrogen atoms per monomer unit
s = length of a specific low molecular weight radical in monomer units
α = transfer coefficient

References and Notes

(1) Gray, M. K.; Zhou, H. Y.; Nguyen, S. T.; Torkelson, J. M. *Macromolecules* **2003**, *36*, 5792−5797.
(2) De Witt, M. J.; Dooling, D. J.; Broadbelt, L. J. *Ind. Eng. Chem. Res.* **1999**, *39*, 2228−2237.
(3) Kruse, T. M.; Woo, O. S.; Wong, H.-W.; Khan, S. S.; Broadbelt, L. J. *Macromolecules* **2002**, *35*, 7830−7844.
(4) Ballesteros, O. G.; Maretti, L.; Sastre, R.; Scaiano, J. C. *Macromolecules* **2001**, *34*, 6184−6187.
(5) Benoit, D.; Grimaldi, S.; Finet, J. P.; Tordo, P.; Fontanille, M.; Gnanou, Y. *Polym. Prepr.* **1997**, *38*, 729−730.
(6) Butte, A.; Storti, G.; Morbidelli, M. *Chem. Eng. Sci.* **1999**, *54*, 3225−3231.
(7) Catala, J. M.; Bubel, F.; Hammouch, S. O. *Macromolecules* **1995**, *28*, 8441−8443.
(8) Goto, A.; Fukuda, T. *Macromolecules* **1997**, *30*, 5183−5186.
(9) Greszta, D.; Matyjaszewski, K. *Macromolecules* **1996**, *29*, 7661−7670.
(10) Le Mercier, C.; Lutz, J. F.; Marque, S.; Le Moigne, F.; Tordo, P.; Lacroix-Desmazes, P.; Boutevin, B.; Couturier, J. L.; Guerret, O.; Martschke, R.; Sobek, J.; Fischer, H. *Controlled/Living Radical Polymerization: Progress in ATRP, NMR and Raft;* ACS Symposium Series 768; American Chemical Society: Washington, DC, 2000.
(11) Lutz, J. F.; Lacroix-Desmazes, P.; Boutevin, B. *Macromol. Rapid Commun.* **2001**, *22*, 189−193.
(12) Shipp, D. A.; Matyjaszewski, K. *Macromolecules* **1999**, *32*, 2948−2955.
(13) Skene, W. G.; Belt, S. T.; Connolly, T. J.; Hahn, P.; Scaiano, J. C. *Macromolecules* **1998**, *31*, 9103−9105.
(14) Souaille, M.; Fischer, H. *Macromolecules* **2000**, *33*, 7378−7394.
(15) Veregin, R. P. N.; Georges, M. K.; Hamer, G. K.; Kazmaier, P. M. *Macromolecules* **1995**, *28*, 4391−4398.

(16) Veregin, R. P. N.; Odell, P. G.; Michalak, L. M.; Georges, M. K. *Macromolecules* **1996**, *29*, 3346−3352.
(17) Hawker, C. J.; Bosman, A. W.; Harth, E. *Chem. Rev.* **2001**, *101*, 3661−3688.
(18) Greszta, D.; Matyjaszewski, K. *Macromolecules* **1996**, *29*, 5239−5240.
(19) Gregg, R. A.; Mayo, F. R. *Discuss. Faraday Soc.* **1947**, *2*, 328−337.
(20) Li, I.; Howell, B. A.; Matyjaszewski, K.; Shigemoto, T.; Smith, P. B.; Priddy, D. B. *Macromolecules* **1995**, *28*, 6692−6693.
(21) He, J.; Li, L.; Yang, Y. *Macromolecules* **2000**, *33*, 2286−2289.
(22) Matyjaszewski, K.; Davis, K.; Patten, T. E.; Wei, M. L. *Tetrahedron* **1997**, *53*, 15321−15329.
(23) Flory, P. *J. Am. Chem. Soc.* **1937**, *59*, 241−253.
(24) Mayo, F. R. *J. Am. Chem. Soc.* **1968**, *90*, 1289−1295.
(25) Buzanowski, W. C.; Graham, J. D.; Priddy, D. B.; Shero, E. *Polymer* **1992**, *33*, 3055−3059.
(26) Souaille, M.; Fischer, H. *Macromolecules* **2002**, *35*, 248−261.
(27) Odian, G. *Principles of Polymerization*, 2nd ed.; John Wiley & Sons: New York, 1981.
(28) Ohno, K.; Tsujii, Y.; Fukuda, T. *Macromolecules* **1997**, *30*, 2503−2506.
(29) Souaille, M.; Fischer, H. *Macromolecules* **2001**, *34*, 2830−2838.
(30) Evans, M. G.; Polanyi, M. *Trans. Faraday Soc.* **1938**, *34*, 11−29.
(31) Marque, S.; Le Mercier, C.; Tordo, P.; Fischer, H. *Macromolecules* **2000**, *33*, 4403−4410.
(32) Fukuda, T.; Goto, A.; Ohno, K. *Macromol. Rapid Commun.* **2000**, *21*, 151−165.
(33) Hui, A. W.; Hamielec, A. E. *J. Appl. Polym. Sci.* **1972**, *16*, 749−769.
(34) Moad, G.; Solomon, D. H. *The Chemistry of Free Radical Polymerization*; Elsevier Science: Oxford, UK, 1995.
(35) Petzold, L. R. *DASSL Differential/Algebraic System Solver*; Sandia National Laboratories: Livermore, CA, 1983.
(36) Wang, M.; Smith, J. M.; McCoy, B. J. *AIChE J.* **1995**, *41*, 1521−1533.
(37) Kodera, Y.; McCoy, B. J. *AIChE J.* **1997**, *43*, 3205−3214.
(38) Teymour, F.; Campbell, J. D. *Macromolecules* **1994**, *27*, 2460−2469.
(39) McCoy, B. J. *AIChE J.* **1993**, *39*, 1827−1833.
(40) Pladis, P.; Kiparissides, C. *Chem. Eng. Sci.* **1998**, *53*, 3315−3333.
(41) Saidel, G. M.; Katz, S. *J. Polym. Sci., Part A-2* **1968**, *6*, 1149−1160.
(42) Woo, O. S.; Broadbelt, L. J. *Catal. Today* **1998**, *40*, 121−140.
(43) Woo, O. S. Resource Recovery of Polystyrene to Monomer Through Binary Mixture Pyrolysis and Base Catalysis. Ph.D. Dissertation, Northwestern University, Evanston, IL, 1999.
(44) Stein, S. E.; Lias, S. G.; Liebman, J. F.; Kafafi, S. A. *NIST Structures and Properties Users Guide*; U.S. Department of Commerce: National Institute of Standards and Technology, 1994 (Jan).
(45) Stewart, W. E.; Caracotsios, M.; Sorensen, J. P. *AIChE J.* **1992**, *38*, 641−650.
(46) Deady, M.; Mau, A. W. H.; Moad, G.; Spurling, T. H. *Makromol. Chem.* **1993**, *194*, 1691−1705.
(47) Brandup, J.; Immergut, E. H.; Grulke, E. A. *Polymer Handbook*, 14th ed.; John Wiley and Sons: New York, 1999.
(48) Fischer, H. *Chem. Rev.* **2001**, *101*, 3581−3610.
(49) Griller, D. In *Radical Reaction Rates in Liquid*; Fischer, H., Ed.; Springer-Verlag: Berlin, 1984; p 12.
(50) Fried, J. R. *Polymer Science and Technology*; Prentice Hall: Upper Saddle River, NJ, 1995.
(51) Schreck, V. A.; Serelis, A. K.; Solomon, D. H. *Aust. J. Chem.* **1989**, *42*, 375−393.
(52) Sobek, J.; Martschke, R.; Fischer, H. *J. Am. Chem. Soc.* **2001**, *123*, 2849−2857.

MA030091V